



OPEN

Parameter estimation on multivalent ITC data sets

Franziska Erlekm, Maximilian Zumbansen & Marcus Weber✉

The Wiseman fitting can be used to extract binding parameters from ITC data sets, such as heat of binding, number of binding sites, and the overall dissociation rate. The classical Wiseman fitting assumes a direct binding process and neglects the possibility of intermediate binding steps. In principle, it only provides thermodynamic information and not the kinetics of the process. In this article we show that a concentration dependent dissociation constant could possibly stem from intermediate binding steps. The mathematical form of this dependency can be exploited with the aid of the Robust Perron Cluster Cluster Analysis method. Our proposed extension of the Wiseman fitting rationalizes the concentration dependency, and can probably also be used to determine the kinetic parameters of intermediate binding steps of a multivalent binding process. The novelty of this paper is to assume that the binding rate varies per titration step due to the change of the ligand concentration and to use this information in the Wiseman fitting. We do not claim to produce the most accurate values of the binding parameters, we rather present a novel method of how to approach multivalent bindings from a different angle.

The Isothermal Titration Calorimetry (ITC) experiment, together with a method to extract binding parameters of binding interactions between a macromolecule and a ligand, was introduced by Wiseman et al. in 1989¹. The assembly of this experiment is a reference cell containing a buffer solution, a main cell containing a fixed macromolecule concentration. Both cells are in an adiabatic jacket. The ligand concentration is titrated through a syringe into the main cell at fixed time points, evolving or absorbing heat during the binding process. In order to maintain the same temperature as in the reference cell, the main cell is heated or cooled down and the power used is being recorded. As the molar ratio between ligand and macromolecule increases with each injection, at some point saturation occurs and the heat evolved decreases. The classical ITC method would then connect the heat peaks to a sigmoidal curve. The curve slope at midpoint is K_d . The midpoint itself is the stoichiometry.

Based on the ITC experiment, another method was introduced in 2012 by Burnouf et al.², as well as Vander Meulen and Butcher³, which not only extracts thermodynamic information, but also binding kinetics from the heat flow. KinITC approximates the exponential curve of every injection of the isotherm after each peak with a least squares method. Finally, the k_{on} of the binding process is determined by averaging the k_{on} rates of all the titration steps.

The method presented in this paper uses the integrated peaks of the recorded heat flow and optimizes the kinetic binding parameters such that the deviation to the actual heat flow is minimal. This method is performed for both the Wiseman fitting and the Q_c fitting. Again we show that the binding rates do differ for the first and subsequent bindings and unbindings. k_{on} is ligand concentration dependent and changes thus over time.

First, the experimental binding rates for each injection can be extracted. The overall *binding rates* k_{on} and k_{off} are retrieved by calculating the average of those experimental binding rates. Their fraction defines the *dissociation constant*

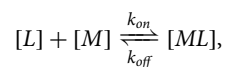
$$K_d := \frac{k_{off}}{k_{on}},$$

as well as the *association constant*

$$K_a := \frac{k_{on}}{k_{off}}.$$

Both are binding parameters extracted by the Wiseman method. The binding rates determine the binding affinity between two molecules. Having a molecule L and a molecule M , a single binding is described by

Zuse Institute Berlin, Takustraße 7, 14195 Berlin, Germany. ✉email: weber@zib.de



where $[\cdot]$ denotes the *free molecule's concentration*.

Recently, a new method was proposed by Erlekm et al.⁴ to retrieve microscopic binding rates through the experimental binding rates extracted via kinITC. Microscopic binding rates determine the binding affinity between the binding sites of two molecules which is not constant. This is the fundamental difference to the existing kinITC method: In the classical kinITC the heat curve of each injection is used to obtain a k_{on} value which is averaged in the end to an overall k_{on} rate of the binding process. For kinITC the shapes of the heat flow peaks are essential, whereas we only need the thermodynamic information, because these reactions are concentration dependent. The key point is that there is a concentration dependent k_{on} rate per titration step.

In⁴, the Robust Perron Cluster Algorithm (PCCA+) is used to coarse grain microscopic binding rates to modelled binding rates for each molar ratio, which are then used to fit the experimental binding rates. The transition states of complex binding processes can be modeled with row-stochastic rate matrices. PCCA+ is a spectral cluster method to reduce the dimensionality of these matrices. The result is a fuzzy clustering and each microstate gets assigned a certain membership to the two macro states: bound and unbound. In⁵ Weber and Röblitz demonstrate that this robust method always delivers a fuzzy clustering for nearly uncoupled Markov chains with transition states. The advantage compared to other clustering methods is that for PCCA+ the process must not necessarily be reversible and the matrix does not need to be decomposable.

This shown concentration dependency of the paper⁴ gave the inspiration for the following: Erlekm et al. showed an interdependence of k_{on} to the ligand concentration. In this paper, we will approach the topic of concentration dependence from another angle. In this paper we assume a dependence of the dissociation rate k_{off} and the ligand concentration.

The thermodynamic binding parameters are the enthalpy or *heat of binding* ΔH° , which defines the amount of heat absorbed or produced for a binding, the *entropy* ΔS° , which is a measure of dispersal of energy for a binding, and the *Gibbs free energy* ΔG° , the amount of available energy, and the *number of binding sites* n . As stated in¹, the heat of binding, the entropy, the Gibbs free energy, and the association constant are related through the following equation

$$\Delta G^\circ = -RT \ln K_a = \Delta H^\circ - T\Delta S^\circ,$$

where R is the gas constant and T the absolute temperature in Kelvin.

In this paper, we will compare the resulting graphs of the Wiseman fitting with the proposed \mathcal{Q}_c fitting of the paper⁴ over ITC data sets. For this proof of concept we used experimental ITC data from Igde et al.⁶. The receptors used therein were lectin Concanavalin A (Con A). Depending on pH of the assay, the receptor can be bivalent or tetravalent. The ligands were glycooligomers based on oligo(amidoamines) with pendant mannose side chains. For the bivalent fitting we use bivalent Con A with the bivalent macromolecule for the bivalent fitting. For the trivalent fitting we used the trivalent Con A and the tetravalent macromolecule. Thus, the maximal compound valency depends on the minimum valency of ligand and receptor. Because we are using the Wiseman function that hold for 1:1 stoichiometries in¹, we also assume a 1:1 stoichiometry in our examples below.

The Wiseman fitting

Having an ITC data set of a binding between ligand L and macromolecule M with $T \in \mathbb{N}$ injections, and the respective *sets of total concentrations* $L_t = \{l_1, \dots, l_T\}$ and $M_t = \{m_1, \dots, m_T\}$, the *Wiseman function* is defined as

$$W(K_a, n; l, m) := \frac{1}{2} \left(1 + \frac{n - \frac{l}{m} - \frac{1}{mK_a}}{\sqrt{\left(n + \frac{l}{m} + \frac{1}{mK_a}\right)^2 - 4n\frac{l}{m}}} \right),$$

for $l \in L_t$ and $m \in M_t$. By using the *integrated peaks of the ITC data for each injection*

$$q_{trans} := \{(q_{trans})_1, \dots, (q_{trans})_T\},$$

the *Wiseman fitting* obtains the association constant, the number of binding site and the enthalpy by minimizing the difference of the hat of binding and the Wiseman function scaled with the enthalpy. For this minimization the Frobenius norm is used:

$$\min_{K_a, n, \Delta H^\circ} \|q_{trans} - W(K_a, n; L_t, M_t) \Delta H^\circ\|. \quad (1)$$

Note, that in this expression the term W is without physical unit. Thus, the unit of q_{trans} will correspond to the physical unit of ΔH° . Scaling q_{trans} just scales ΔH° . In order to be without physical unit, K_a has to reverse the physical unit of m . A common rescaling of m and l only changes the physical unit of K_a .

The \mathcal{Q}_c fitting

As the existing methods^{2,4} suggest, it is valid for multivalent data sets to assume a connection between molar ratio and association or dissociation. With this in mind, a new fitting can be specified by using *microscopic binding rates* for an s -valent binding

k_{on_1} and k_{off_1} for the first microscopic binding,
 k_{on_2} and k_{off_2} for the second consecutive microscopic binding,
 \vdots
 k_{on_s} and k_{off_s} for the s -th consecutive microscopic binding,

for $s \in \mathbb{N}$. To retrieve association constants for each molar ratio, the PCCA+ algorithm from Weber⁵ is used to coarse grain a transition rate matrix of the microscopic binding rates Q to a matrix Q_c containing the (macroscopic) binding rates. The details of how to obtain a dimension reduction via coarse graining is described in⁷. It is important to mention here, that this type of analysis just provides the relative ratios of the rates, but can not figure out the absolute physical unit of them. Thus, providing the k_{on} and k_{off} values with physical units does not make sense here. Following the method of⁴, the bivalent transition rate matrix is

$$Q^T = \begin{pmatrix} -4\alpha & k_{off_1} & k_{off_1} & k_{off_1} & k_{off_1} & 0 & 0 \\ \alpha & -\beta & 0 & 0 & 0 & k_{off_2} & 0 \\ \alpha & 0 & -\beta & 0 & 0 & 0 & k_{off_2} \\ \alpha & 0 & 0 & -\beta & 0 & k_{off_2} & 0 \\ \alpha & 0 & 0 & 0 & -\beta & 0 & k_{off_2} \\ 0 & k_{on_2} & 0 & k_{on_2} & 0 & -2k_{off_2} & 0 \\ 0 & 0 & k_{on_2} & 0 & k_{on_2} & 0 & -2k_{off_2} \end{pmatrix}, \quad (2)$$

with $\alpha := k_{on_1}[L]$, $\beta := -k_{off_1} - k_{on_2}$. For the trivalent case, see the Supplementary File. To get from the transposed transition rate matrix Q^T to its coarse grained transposed counterpart Q_c^T , the PCCA+ algorithm introduces

$$Q_c^T = (\chi^T \Pi \chi)^{-1} \chi^T \Pi Q^T \chi,$$

where $\Pi := \text{diag}(\pi)$ with stationary distribution π of the state space S related to Q , and fuzzy membership matrix χ . To retrieve χ , the inner simplex algorithm from⁸ is used. By using the interpretation of Weber⁹, the coarse grained matrix yields

$$Q_c^T = \begin{pmatrix} -k_{on}[L] & k_{off} \\ k_{on}[L] & -k_{off} \end{pmatrix},$$

from which K_a can be retrieved.

The transition rate matrix Q requires the ligand concentration $[L]$, which will be calculated iteratively for each injection i as

$$[L]_i = \begin{cases} l_i, & \text{if } i = 1, \\ [L]_{i-1} + l_i - (L_b)_{i-1}, & \text{otherwise,} \end{cases}$$

where

$$(L_b)_i := \frac{nm_i + l_i + \frac{1}{K_a} - \sqrt{\left(nm_i + l_i + \frac{1}{K_a}\right)^2 - 4nm_i l_i}}{2}$$

is the *bound ligand concentration for injection i* . For an s -valent binding, we denote

$$Q(k_{on_1}, k_{off_1}, \dots, k_{on_s}, k_{off_s}; [L]) = K_1, \dots, K_T,$$

with the set of free ligand concentrations $[L]$ and, on the right side, the resulting association constants K_i for each injection $i \in \{1, \dots, T\}$. With the Frobenius norm, we then define the Q_c fitting as

$$\min_{\substack{k_{on_1}, \dots, k_{on_s} \\ k_{off_1}, \dots, k_{off_s} \\ n, \Delta H^\circ}} \|q_{trans} - W(Q(\dots; [L]), n; L_t, M_t) \Delta H^\circ\|. \quad (3)$$

Extracting the experimental data

To extract the total concentrations L_t and M_t from the ITC experiments, we follow the supporting information's appendix I of Egawa et al.¹⁰, where

$$l_i = c_L \left(\sum_{k=1}^i V_k \right) \frac{2V_0 - \sum_{k=1}^i V_k}{2(V_0)^2}$$

$$m_i = c_M \frac{2V_0 - \sum_{k=1}^i V_k}{2V_0 + \sum_{k=1}^i V_k},$$

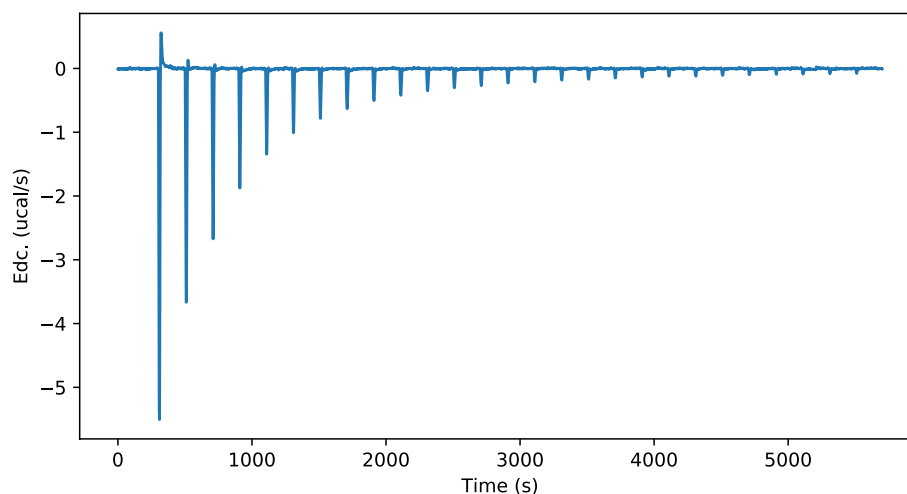


Figure 1. Plot of the deconvolved power trace (Edc) of bindings between a decavalent Con A and a bivalent precision glycomacromolecule over time and through 14 injections.

with main cell volume V_0 , containing the macromolecules, successive injected volumes V_i , $i \in \{1, \dots, T\}$, containing the ligands, and concentrations of ligand c_L and of macromolecule c_M . Thus, the total volume is $V_{Tot} = V_0 + \sum_{i=1}^T V_i$.

For the bivalent case, the values are

$$\begin{aligned} c_M &= 0.071 \text{ mmol/l} & V_0 &= 1.442 \text{ ml} \\ c_L &= 0.7 \text{ mmol/l} & V_1 &= 0.001 \text{ ml}, & V_j &= 0.01 \text{ ml}, \end{aligned}$$

and for the trivalent case

$$\begin{aligned} c_M &= 0.0918 \text{ mmol/l} & V_0 &= 1.442 \text{ ml} \\ c_L &= 0.978 \text{ mmol/l} & V_1 &= 0.001 \text{ ml}, & V_j &= 0.01 \text{ ml}, \end{aligned}$$

with $j \in \{2, \dots, 14\}$. In the following, we will compare the quality between the Wiseman fitting and the proposed Q_c fitting.

Comparison of fittings

For the Wiseman fitting, the peaks of the heat curve are integrated with univariate splines of degree 5. The parameters K_a , n and ΔH° are obtained by a Nelder-Mead minimization.

For the Q_c fitting, the algorithm is implemented as a random search loop with breaking condition when a better norm, compared to the Wiseman fitting, is found. When a suitable norm threshold is reached, a Nelder-Mead minimization is applied on the Q_c fitting over parameters n and ΔH° to find the optimal solution to the current microscopic binding rates.

In the following subsection we present the Wiseman fitting to experimental data from Igde et al.⁶ In this work, the authors selected data sets of bi- and trivalent ligands binding to tetrameric Con A with four binding sites from a series of measurements. The precision glycomacromolecule were mannose ligands with oligomer scaffolds. Since we assume a 1:1 stoichiometry, the binding process can only have the valency of the respective ligand, no matter if the receptor has more potential binding sites.

Bivalent ligand case. The bivalent case, where Con A and a bivalent precision glycomacromolecules bind together, resolves into the ITC plot as depicted in Fig. 1:

The heat evolved is extracted by integration over the 14 injection peaks. The Wiseman fitting returns the following binding parameters

$$\begin{aligned} K_a &= 93.3295 & n &= 0.1998 \\ \Delta H^\circ &= -132.3069 \text{ kcal/mol} \end{aligned}$$

and results in an error of 5.4838.

For the Q_c fitting, the retrieved binding parameters are

$$\begin{aligned} k_{on1} &= 136.4185 & k_{off1} &= 2.3716 \\ k_{on2} &= 33.4088 & k_{off2} &= 18.5925 \\ n &= 0.3208 & \Delta H^\circ &= -73.4629 \text{ kcal/mol} \end{aligned}$$

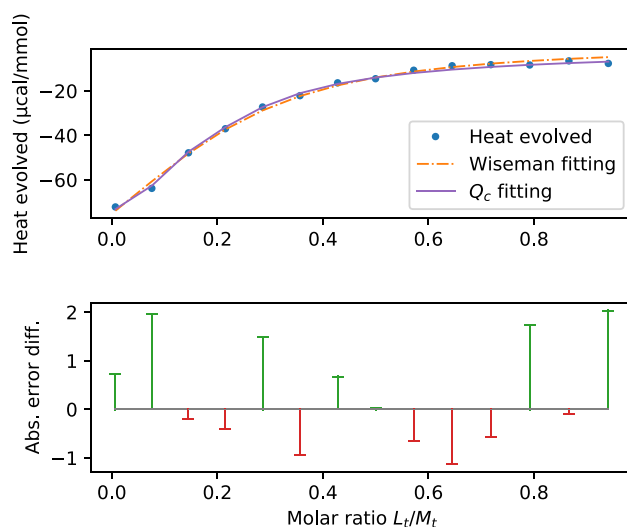


Figure 2. (a) Integrated heat per injection over molar ratio with Wiseman graphs of Wiseman and Q_c fitting for the bivalent case. (b) Difference of absolute error plots from Wiseman and Q_c fitting.

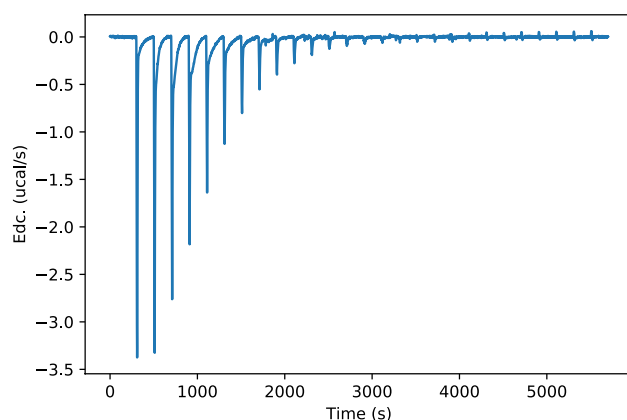


Figure 3. Plot of the deconvolved power trace (Edc) of bindings between a trivalent Con A and a tetravalent precision glycomacromolecule over time.

The error for this fitting is 3.435. The results of the Q_c and the Wiseman fitting is shown in Fig. 2(a). Their respective errors are shown in Fig. 2(b).

When comparing the binding parameters, the heat of binding ΔH° from the Wiseman fitting is almost double the value from the Q_c fitting, whereas the number of sites n is only two thirds.

The expected value for n is 0.2, which is better represented through the Wiseman fitting.

The association constant K_a is not comparable to the microscopic association constants

$$K_1 := k_{on1}/k_{off1} = 57.5217$$

$$K_2 := k_{on2}/k_{off2} = 1.7969.$$

The latter signal a stronger first and a very weak second binding. As has been said before: Because of the lack of physical units, the analysis just allows for this “relative”, qualitative result.

Trivalent ligand case. We will now examine the ITC plot resulting from a binding between a trivalent Con A and a tetravalent Precision Glycomacromolecule, as depicted in Fig. 3.

Compared to the bivalent case, the heat curve resolves in a distinct slope at molar ratio 0.3. As the slope is the most crucial part when determining the binding constants, before using the Frobenius norm, the absolute difference between fitting and q_{trans} is multiplied by a Gaussian curve with mean $\mu = 0.3$ and standard deviation $\sigma = 0.1758$. The first injection is considered an outlier and is excluded from the minimization.

For the Wiseman fitting, the resulting binding parameters are

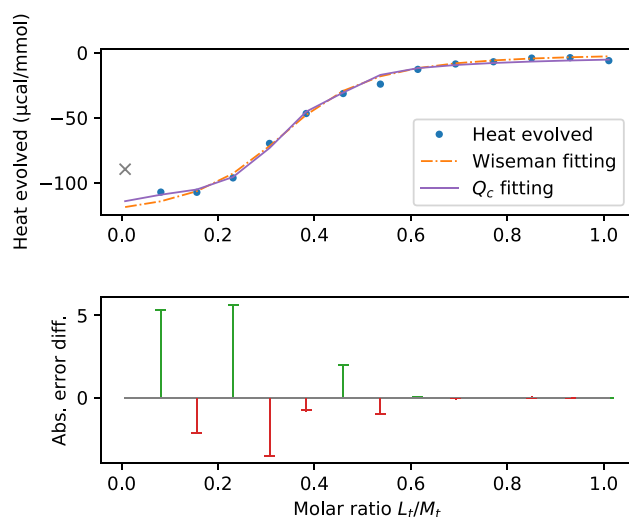


Figure 4. (a) Integrated heat per injection over molar ratio with Wiseman graphs of Wiseman and Q_c fitting for the trivalent case. (b) Difference of absolute error plots from Wiseman and Q_c fitting. Calculated with a Gaussian distribution to apply weight around the slope.

$$K_a = 410.2917 \quad n = 0.3586$$

$$\Delta H^\circ = -127.7664 \text{ kcal/mol,}$$

and the error is 13.1455.

The Q_c fitting results in binding parameters

$$k_{on1} = 559.1484 \quad k_{off1} = 1844.5886$$

$$k_{on2} = 489.7665 \quad k_{off2} = 81.966$$

$$k_{on3} = 1056.7834 \quad k_{off3} = 1338.633$$

$$n = 0.3624 \quad \Delta H^\circ = -115.1639 \text{ kcal/mol}$$

with an error of 11.1979. The results of the Q_c and the Wiseman fitting are shown in Fig. 4(a). Their respective errors are shown in Fig. 4(b).

This time the number of sites n is almost identical for both fittings and the heat of binding is fairly equal.

For the microscopic association constants, we have

$$K_1 = 0.3031 \quad K_2 = 5.9752 \quad K_3 = 0.7894,$$

which are very low numbers compared to K_a from the Wiseman fitting. The second binding appears to be the easiest, whereas the first and the last are less frequent.

Model selection

There is not much freedom of determining the correct model for the interpretation of the experimental data. The Wiseman fitting itself is assumed to be the fixed root model for the interpretation of the ITC data in terms of association and dissociation constants. The model Q for the detailed kinetic process depends on the chemical nature of the substances. The elementary binding events (the stoichiometry) only depend on the number of binding sites and ligand sites

The only free choice we made is to project the matrix Q to a two-dimensional matrix Q_c , because we assume that the only dominating process is the “slow” overall binding event, which we hope to model correctly and robustly by the coarse grained matrix.

The choice of the projection space has been discussed in terms of “implied timescales”. It has been analyzed in terms of the separation of the timescale of the projected process with regard to the next faster process¹¹. The first eigenvalue λ_1 of the Q_c -matrix is always 0, thus this separation of timescales can be estimated from taking the ratio of the second and third eigenvalue of Q_c , $\frac{\lambda_2}{\lambda_3}$. In case of the bivalent example, this ratio grows from 1.1 in the first titration step to 2 in the last titration step, which means that the second faster process is already two times faster than the slowest one (at the end of the ITC experiment). This indicates a good separation and choice of modelling. In the case of the trivalent example, however, this ratio is always at about 1.14 and indicates a bad separation.

If we would model Q_c as a two-step binding process instead of a one-step binding, then the timescales separation would be given by the ratio of the third and fourth eigenvalues of Q , i.e. $\frac{\lambda_4}{\lambda_3}$. In this case this ratio grows from 1.0 in the first titration step to 4.7 in the last one along the ITC experiment. However, this would not allow for a comparison with regard to the applied Wiseman fitting.

Error Estimates

To test the robustness of this fitting, the ITC input data was disturbed by up to 1%, i.e. every value was multiplied by a random variable $x_i \in [0.99, 1.01]$.

In the bivalent example we have the following changes after disturbing the input: n is 0.33% higher, ΔH decreased by 0.31% and the best norm decreased by 0.18% compared to the undisturbed model. The k_{on1} , k_{on2} , k_{off1} and k_{off2} differ only by a factor of 10^{-6} from the disturbed model binding parameters. Therefore, K_1 and K_2 do not differ either. Thus, we have a stable model for the bivalent case.

The trivalent case is more complicated. The binding parameters of the undisturbed and undisturbed models differ up to 743%. K_1 , K_2 and K_3 therefore also differ substantially, up to 653%. However, with the different optimum found in the disturbed setting, the stoichiometry and the heat of binding are similar. In the disturbed example, n is only 0.04% higher, ΔH decreased by 1.5% and the best norm decreased by 1.36% compared to the undisturbed model. To summarize, for the trivalent binding, the Q_c fitting may not deliver satisfying results. This may be due to the same reason that we discovered in the spectral gap analysis. Possibly, the Wiseman fitting is not suitable for trivalent bindings, because there are actually three macro states instead of two. For the Q_c fitting, this is an interesting insight, because for trivalent bindings we would need to project onto a 3×3 clustered rate matrix instead of a 2×2 matrix.

Conclusion

In this paper we have shown the Q_c and the Wiseman fitting for two numerical examples. We conclude that with PCCA+ the fitting of binding parameters of bivalent and trivalent ligands is better in terms of absolute errors than the Wiseman fitting. We demonstrated the results of particular association constants for each subsequent binding step. The major advantage of the proposed method is to gain kinetic information of each binding step rather than for the whole binding process only. However, the binding parameters are just “qualitative” not quantitative. Whereas, kinetic ITC assumes concentration independent binding associations. Our method makes use of the systematic change of the association “constants” along the measurements.

Outlook

By taking microscopic binding and concentrations into account, we have proven the existence of a better fitting of bivalent and trivalent ITC data sets. However, the current algorithm for the Q_c fitting utilizes random search to find the binding parameters. An algorithm for an optimal solution is currently not available and remains a problem for future research.

As the resulting fitting relies on a transition matrix and the interpretation of its coarse grained counterpart, the approach of this paper could contribute to a model which is able to explain even more complex heat curves, where the Wiseman graph is no longer satisfactory.

Our paper only shows a proof of concept for a bivalent and a trivalent model. In the future the algorithm can be tested for bindings of higher valencies to learn more about its limitations.

Further, we have assumed a 1:1 stoichiometry that does not necessarily occur in all molecular binding experiments. The theory could therefore be generalized for other stoichiometries as a future piece of research.

Lastly, as a goodness of fit metric we used the fitting error. The two models could be further compared using different criteria, such as the Bayesian information criterion. Apart from that, a parameter study can be of interest to show which of the binding parameters are correlated.

Data availability

The data and the algorithm that support the findings of this study are openly available at <https://github.com/mazumba/si-multivalent-params>.

Received: 4 October 2021; Accepted: 21 July 2022

Published online: 04 August 2022

References

1. Wiseman, T., Williston, S., Brandts, J. F. & Lin, L.-N. Rapid measurement of binding constants and heats of binding using a new titration calorimeter. *Anal. Biochem.* **179**, 131–137 (1989).
2. Burnouf, D. *et al.* Kinitc: A new method for obtaining joint thermodynamic and kinetic data by isothermal titration calorimetry. *J. Am. Chem. Soc.* **134**, 559–565 (2012).
3. Vander Meulen, K. A. & Butcher, S. E. Characterization of the kinetic and thermodynamic landscape of rna folding using a novel application of isothermal titration calorimetry. *Nucleic Acids Res.* **40**, 2140–2151 (2012).
4. Erlekam, F., Igde, S., Röblitz, S., Hartmann, L. & Weber, M. Modeling of multivalent ligand-receptor binding measured by kinitc. *Computation* **7**, 46 (2019).
5. Röblitz, S. & Weber, M. Fuzzy spectral clustering by pcca+: Application to markov state models and data classification. *Adv. Data Anal. Classif.* **7**, 147–179 (2013).
6. Igde, S. *et al.* Supporting information—linear precision glycomacromolecules with varying interligand spacing and linker functionalities binding to concanavalin a and the bacterial lectin fimh.
7. Kube, S. & Weber, M. A coarse graining method for the identification of transition rates between molecular conformations. *J. Chem. Phys.* **126**, 024103 (2007).
8. Weber, M. & Galliat, T. Characterization of transition states in conformational dynamics using fuzzy sets. (2002).
9. Weber, M. Implications of pcca+ in molecular simulation. *Computation* **6**, 20 (2018).
10. Egawa, T., Tsuneshige, A., Suematsu, M. & Yonetani, T. Method for determination of association and dissociation rate constants of reversible bimolecular reactions by isothermal titration calorimeters. *Anal. Chem.* **79**, 2972–2978 (2007).

Acknowledgements

This study was partially supported by CRC 765, project C2 "Non-Equilibrium Kinetics of Multivalent Binding".

Author contributions

F.E. developed the theoretical background of concentration dependent binding rates and wrote parts of the paper. M.Z. conducted the Wiseman fitting and wrote parts of the paper. M.W. developed the PCCA+ algorithm and wrote parts of the paper. All authors reviewed the manuscript.

Funding

Open Access funding enabled and organized by Projekt DEAL.

Competing interests

The authors declare no competing interests.

Additional information

Supplementary Information The online version contains supplementary material available at <https://doi.org/10.1038/s41598-022-17188-x>.

Correspondence and requests for materials should be addressed to M.W.

Reprints and permissions information is available at www.nature.com/reprints.

Publisher's note Springer Nature remains neutral with regard to jurisdictional claims in published maps and institutional affiliations.



Open Access This article is licensed under a Creative Commons Attribution 4.0 International License, which permits use, sharing, adaptation, distribution and reproduction in any medium or format, as long as you give appropriate credit to the original author(s) and the source, provide a link to the Creative Commons licence, and indicate if changes were made. The images or other third party material in this article are included in the article's Creative Commons licence, unless indicated otherwise in a credit line to the material. If material is not included in the article's Creative Commons licence and your intended use is not permitted by statutory regulation or exceeds the permitted use, you will need to obtain permission directly from the copyright holder. To view a copy of this licence, visit <http://creativecommons.org/licenses/by/4.0/>.

© The Author(s) 2022